10,11

Effect of vacancy defects on the electronic and electrophysical properties of quasi-2D graphene/nanotube films: DFTB study

© M.M. Slepchenkov

Saratov National Research State University,
Saratov, Russia

E-mail: slepchenkovm@mail.ru

Received July 9, 2025
Revised July 13, 2025
Accepted July 23, 2025

Quasi-2D hybrid carbon films formed by horizontally oriented single-walled zigzag (10,0) nanotubes sandwiched between two graphene sheets and covalently bonded to them have been studied within the density functional based tight binding method. The effect of single-vacancy defects on the electronic and electrophysical properties of hybrid graphene-nanotube films has been analyzed. It has been found that both defect-free and defective hybrid films are characterized by the presence of an energy gap in the band structure. With the appearance of defects and an increase in their number, the energy gap begins to narrow. Partial charge transfer from the nanotube to the graphene sheets has been revealed. The charge transfer increases with the appearance of defects and leads to an increase in the anisotropy of electrical conductivity in hybrid graphene-nanotube films.

Keywords: single vacancy defect, density of electron states, electrical conductivity, charge transfer.

DOI: 10.61011/PSS.2025.07.61871.180-25

1. Introduction

Graphene and carbon nanotubes (CNT) have been the most discussed allotropic modifications of carbon for several decades [1,2]. Combination of graphene and nanotubes into a hybrid structure stimulated a new stage of development for the fundamental studies and applied design in the field of carbon nanomaterials [3–8]. The growing interest of the researchers in the graphene-nanotube hybrid structures is explained by the ability to produce nanomaterials on their basis with the new and/or improved properties, which exceed the properties of each of the carbon components separately, thanks to the synergistic effect [9–11]. The most frequently used methods for synthesis of hybrid graphene-CNT nanomaterials are the method of layer-by-layer self-assembly [12], sol-gel technology [13], chemical vapor deposition [14], hydrothermal method [15] and physical mixing method [16]. Due to the variety of the synthesis technology it is possible to form the hybrid graphene-CNT nanomaterials with different architecture, including with the different mutual arrangement of graphene layers and nanotubes in the hybrid [17]. The object of many applied studies are the hybrid graphene-CNT nanomaterials with architecture that contains horizontally-aligned nanotubes enclosed between the graphene sheets. The advantages of this architecture are 1) prevention of graphene layers aggregation and 2) solution to the problem of low conductivity of graphene in the perpendicular direction by placement of the conductor with the separators in the form of CNTs [18]. Using hybrid graphene-CNT nanomaterials with horizontally-aligned nanotubes, such devices are created as supercapacitors [19], photodetectors [20], sensors [21].

To control the properties of graphene-CNT nanomaterials, it is important to have information on the patterns of the physical processes happening in them at the atomic-molecular and quantum levels. Therefore the prognostic studies are becoming highly sought regarding mechanical, transport, electronic and optical properties of hybrid graphene-CNT nanostructures being conducted by the methods of atomistic modelling [3,4,22–24]. In particular, paper [22] within the density functional theory (DFT) and non-equilibrium Green's functions method (NEGF) conducted the studies of electric and electronic properties of the hybrid graphene-single-wall CNT (SWCNT) system comprising one SWCNT (5,5), two SWCNTs (8,0) and graphene flakes of various concentration. It was found that as the concentration of graphene flakes increases, the DOS value of the hybrid graphene-SWCNT system at Fermi level increases, which causes the growth of its conductance and current. Studies by the density functional tight-binding method (DFTB) of electronic and transport properties of lateral 2D-1D-2D hybrid structures representing the continuous connection of graphene sheets via a fragment of SWCNT of „zigzag" type of different diameter were carried out in paper [23]. The authors demonstrated the strong nonlinearity in the behavior of the transmission ratio near Fermi energy for such structures depending on the SWCNT diameter. In paper [24] the DFTB and NEGF methods were used to study the problems of quantum transport of electrons through the hybrid carbon structure with the horizontally-aligned SWCNTs of different type of conductivity on the graphene sheet at variable distances between it and the nanotubes. The researchers found different behavior of the drain current for graphene-SWCNT

hybrids with semiconductor and metal nanotubes with the reduction of the distance between the carbon components. For semiconductor SWCNTs the current increases at low bias voltages and decreases at high bias voltages; for the metal SWCNTs the current decreases in the entire considered range of the bias voltage values. At the same time the available theoretical papers studying electronic and electroconductive properties of hybrid graphene-CNT nanomaterials do not consider the effect of structural defects, in particular, point (zero-dimensional) defects of the crystalline lattice that may be formed in the process of graphene and nanotubes synthesis.

The objective of this paper is to study the electronic and electroconductive properties of hybrid graphene-CNT nanomaterials containing point defects of crystalline lattice using atomistic modeling methods. The object of the study are quasi-2D films formed by horizontally-aligned SWCNTs of zigzag type with chirality indices (10,0), enclosed between graphene sheets and covalently bonded thereto. A point defect is a defect of a single vacancy type formed in the atomic lattice of graphene. Such defect is common in graphene synthesis [25]. The selection of SWCNTs of zigzag type is provided for by the fact that to form the covalent bonds with graphene, first of all, such tubes are specifically suitable, as it was shown in paper [26]. The diameter of the selected SWCNT (10,0) is ~ 0.8 nm and complies with the known experimental data on the most frequently synthesized SWCNTs [27].

2. Methods and approaches

The atomic structure and electron-energy characteristics (bond energy E_b, density of electron states (DOS), Fermi level E_F) of the studied hybrid graphene-SWCNT (10,0)-graphene nanostructures were calculated within the DFTB method [28] in the software suite of open access DFTB+ [29]. The selection of the DFTB method is caused by the fact that the crystalline cells (super cells) of the studied hybrid nanostructures contain up to 288 atoms, which increase the labor intensiveness of electron quantum transport calculations therefor. In its turn the DFTB method is approximately three orders faster than DFT. In paper [30] using the graphene example it is shown that the DFTB method may successfully reproduce the geometric and energy characteristics of carbon nanostructures comparable in accuracy to the results of calculation using the DFT method, but with lower computing costs. An optimization was performed to obtain the equilibrium configuration of supercells which consisted in solving the minimax problem for identifying the global minimum of total energy by varying the coordinates of all atoms and the lengths of the translation vectors. The distribution of the electron charge density over atoms is determined in accordance with the Mulliken population analysis [31]. The electrical conductivity of the studied structures was calculated within the framework of the Landauer-Butticker formalism [32] according to the following formula

$$G = 2e^2/h \int_{-\infty}^{\infty} T(E)F_T(E - E_F)dE, \tag{1}$$

where $T(E)$ — average electron transmission function, E_F — Fermi level of the electrodes, e^2/h — quantum of conductivity, F_T — function of thermal broadening of energy levels, defined as

$$F_T = \frac{1}{4k_BT}\,\mathrm{sech}^2\Big(\frac{E - E_F}{2k_BT}\Big), \tag{2}$$

where k_B — Boltzmann constant; T — temperature.

The electron transmission function $T(E)$ is expressed as follows

$$T(E) = Tr\big(\Gamma_S(E)G_C^A(E)\Gamma_D(E)G_C^R(E)\big), \tag{3}$$

where $G_C^A(E)$ and $G_C^R(E)$ — advanced and retarded Green's matrices describing the interaction of the simulated system with electrodes, and $\Gamma_S(E)$ and $\Gamma_D(E)$ — broadening matrices of energy levels of the source and drain electrodes. The electroconductive characteristics were calculated at temperature of 300 K and with the reciprocal space partition using fifty k-points in the direction perpendicular to the current transport direction.

3. Results

Figure 1 shows the initial super cell of quasi-2D graphene-SWCNT (10,0)-graphene film not containing single vacancy defects prior to optimization (Figure 1, *a*) and after optimization (Figure 1, *b*) of the atomic structure. You can see well that in process of optimization both the graphene sheets and the nanotube (10,0) underwent the deformation of the atomic grid, the results of which are the wave-shaped bend of graphene and the extended ellipsoidal shape of the nanotube (compression degree of 1.62). The length of covalent bond between graphene and SWCNT (10,0) is 1.62 A for the optimized super cell with the translation vectors $L_x = 17.22$ A and $L_y = 12.78$ A.

Further defects of single vacancy were added to the atomic structure of the super cell of the hybrid graphene-SWCNT (10,0)-graphene film. The defects were formed in the atomic lattice of graphene sheets. The cases were considered with one, two, three and four defects. Figure 2 shows the optimized super cells of the hybrid graphene-SWCNT (10,0)-graphene film with the different quantity of vacancy defects. Each of the built super cells was tested for thermodynamic stability, which was assessed by the value of the bond energy E_b, calculated according to the formula

$$E_b = E_{hs} - (E_{gr} + E_{CNT}), \tag{4}$$

where E_{hs} — energy of hybrid graphene-SWCNT (10,0)-graphene film, E_{gr} — energy of graphene layers, E_{CNT} —

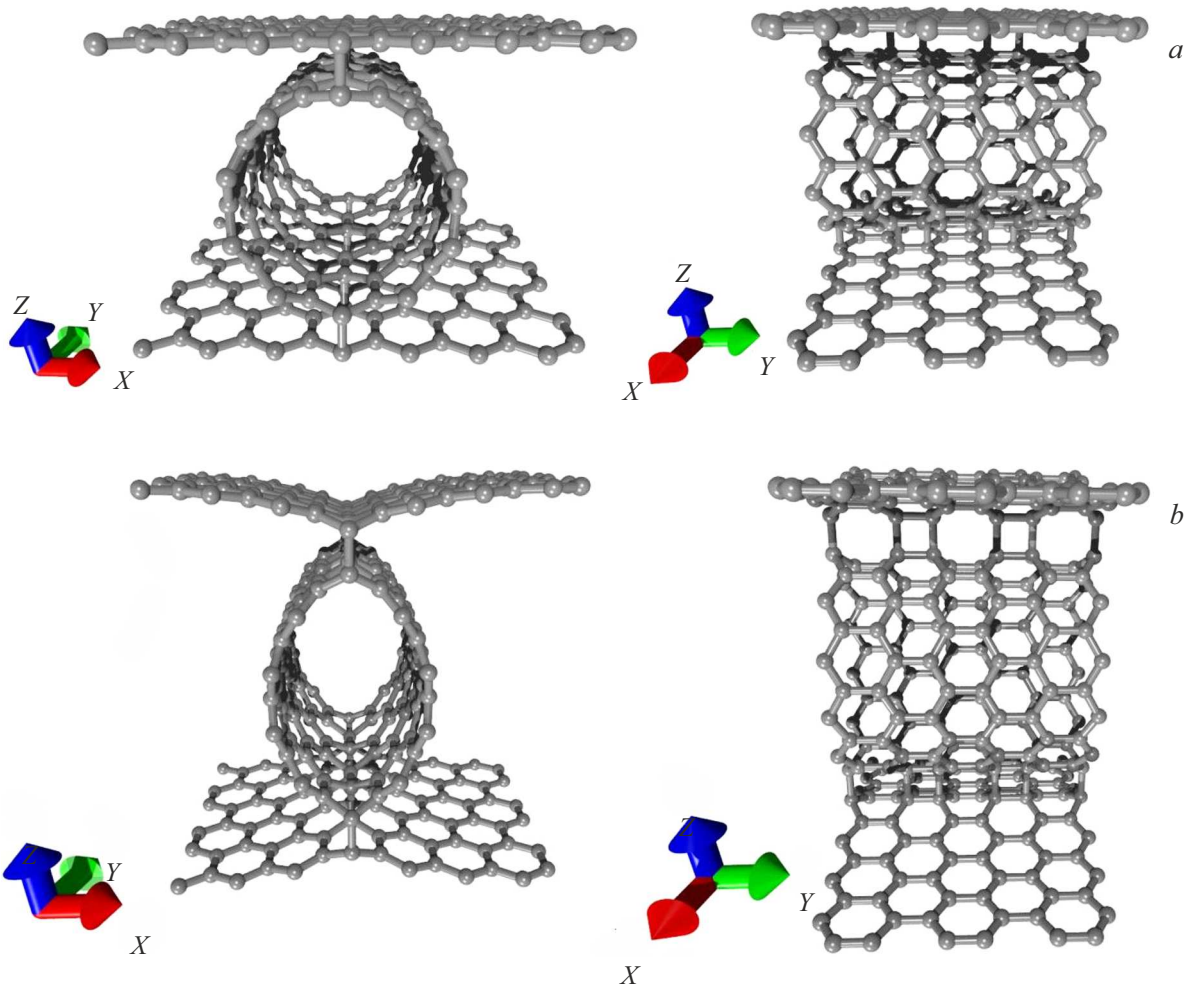

Figure 1. Super cell of hybrid graphene-SWCNT (10,0)-graphene film prior to optimization (a) and after optimization (b) of atomic structure. The front view is shown on the left, and the side view — on the right.

energy of SWCNT (10,0). The hybrid film structure was configured so that its full energy by absolute value was lower than the sum of the full energies of graphene sheets and SWCNT (10,0). The results of the calculation made according to formula (4), showed that the value E_b for super cells of the hybrid graphene-SWCNT (10,0)-graphene film with the growth of the number of single vacancy defects varies in the range of $-15.05 \div -6.23$ eV. The negative value of the bond energy indicates that all super cells of the defective hybrid film are thermodynamically stable. For a super cell of the defect-free hybrid film, the value E_b is -15.06 eV. It should be noted that other variants of single vacancy defect placement in the atomic lattice of graphene sheets were considered: diagonal location of one defect on the upper and one defect on the lower sheets of graphene, two defects on the upper sheet of graphene and no defects on the lower sheet, two defects on the lower sheet of graphene and no defects on the upper sheet. However, the cases presented in Figure 2 are characterized with the value E_b of highest modules, therefore they were selected for further analysis of electronic and electrophysical properties of hybrid graphene-SWCNT (10,0)-graphene films.

Electronic properties of hybrid graphene-SWCNT (10,0)-graphene films were analyzed using distributions of DOS built using the band structure estimation results. All estimates were carried out in the *sp*-basis of atomic orbitals, since the considered hybrid films with the covalently bonded nanotube and graphene include the states with sp^3-hybridization. Figure 3 shows DOS curves for super cells of graphene-SWCNT (10,0)-graphene films with the different number of single vacancy defects and for the defect-free films (in the insert). For demonstration, the energy interval near the Fermi level is selected E_F, since the determinant contribution to the conducting properties of the nanomaterial is made specifically by the electron states at Fermi level. The Fermi level values E_F for each of the calculated super cells are given in Table 1. As you can see from Figure 2, both the hybrid graphene-SWCNT (10,0)-graphene film that contains no defects and the film that contains single vacancy defects are characterized by the presence of the energy interval with zero DOS near the

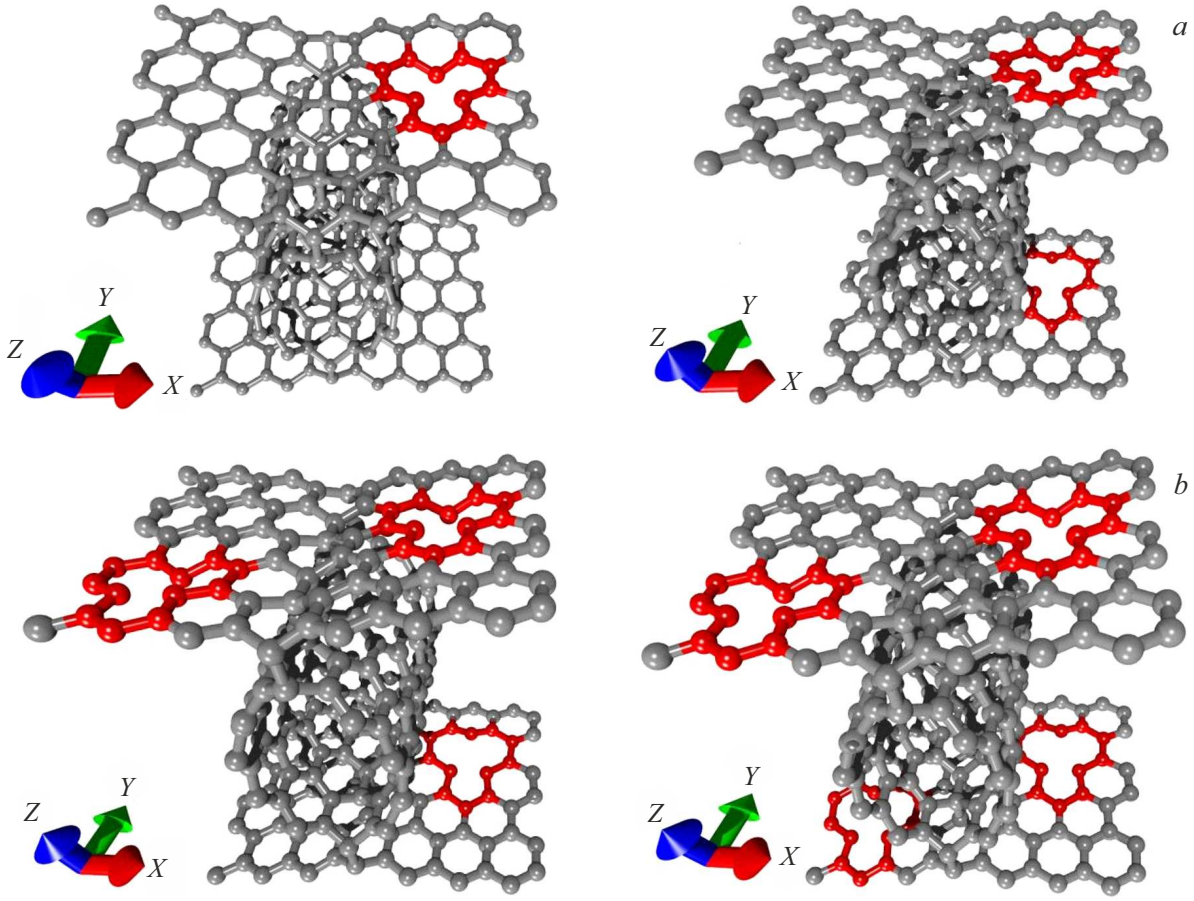

Figure 2. Super cell of hybrid graphene-SWCNT (10,0)-graphene film with the defects of single vacancy type formed in the atomic lattice of graphene sheets: one (a), two (b), three (c) and four (d) defects. The red color shows the defect localization areas.

Fermi level, indicating the opening if an energy gap between the valence band and the conduction band in the band structure. Appearance of the energy gap is provided for by the presence of sp^3-hybridized atoms of carbon participating the formation of a covalent bond between graphene and SWCNT (10,0). The value of the energy gap E_{gap} of defect-free and defective films is given in Table 1. From Figure 3 and Table 1 it follows that with appearance of the defect of single vacancy type in the atomic lattice of graphene the energy gap of the hybrid film narrows down, besides, even if there is one defect only it decreases by more than 2 times, and if there are three and four defects — 3 times. The Fermi level with appearance of the defects moves along the energy axis to the left, staying at the same time in the middle of the narrowing band gap.

Narrowing of the energy gap of the hybrid graphene-SWCNT (10,0)-graphene film with the appearance of defects may be explained from the position of the charge transfer in the graphene-SWCNT (10,0)-graphene system. Figure 4 shows the calculated distributions of partial charge by Mulliken for the atoms of super cells in defect free and defective (containing 1 defect) hybrid films. You can see that in absence of defects (Figure 4, a) the highest

Table 1. Electron-energy characteristics of defect-free and defective hybrid graphene-SWCNT (10,0)-graphene film

Number of defects	E_F, eV	E_{gap}, eV
0	−4.70	0.57
1	−4.87	0.24
2	−4.87	0.23
3	−4.89	0.19
4	−4.89	0.19

redistribution of the partial charge is observed in the area of covalent bond formation between the graphene sheets and the nanotube. Besides, the total charge flows from the nanotube to the graphene sheets with the value of the order of $0.09e$ (e — electron charge). The presence of even one defect (Figure 4, b) results in the fact that the highest redistribution of the partial charge happens in the area of the single vacancy formation. The transfer of the charge between the graphene and nanotube is also more intense within the hybrid film: the total charge with the value of $0.16e$ is transferred to graphene. With the

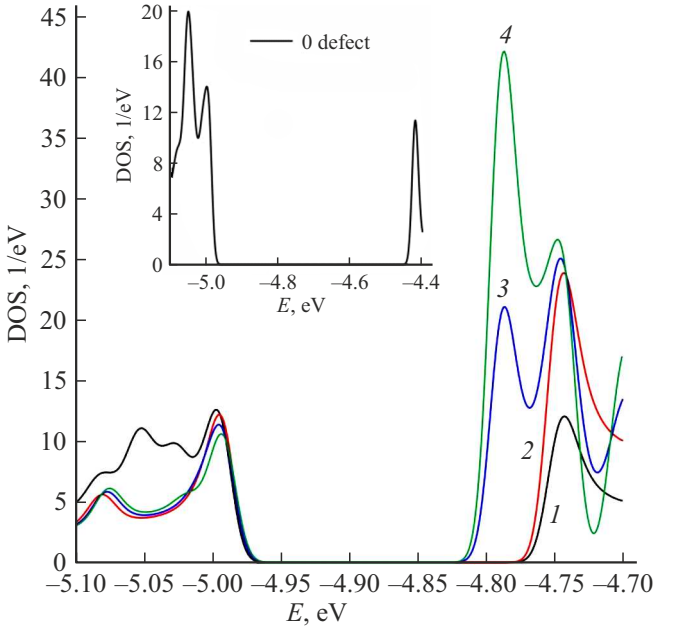

Figure 3. DOS curves of super cells of hybrid graphene-SWCNT (10,0)-graphene film with single vacancy type defects formed in the atomic lattice of graphene sheets: curve *1* — one defect, *2* — two defects, *3* — three defects and curve *4* — four defects. The insert to the figure shows the DOS curve for the super cell of the defect-free hybrid graphene-SWCNT (10,0)-graphene film.

growth of the number of defects the value of the partial charge transferred to graphene increases: with two defects it is $0.21e$, with three defects — $0.25e$, with four defects — $0.28e$. The pattern of partial charge distribution by Mulliken in the atoms of super cells of the hybrid film with two, three and four defects is similar to the case with a single defect.

Electrophysical properties of the studied hybrid graphene-SWCNT (10,0)-graphene films were assessed using the value of electrical conductivity calculated for the two directions of current transport: zigzag (G_x) and armchair (G_y) of the hexagonal lattice of graphene. Calculated values of electrical conductivity of defect-free and defective hybrid films are given in Table 2. Having analyzed the tabular data, it is possible to note that the hybrid graphene-SWCNT (10,0)-graphene films, as well as the graphene are characterized by the anisotropy of conductivity: value G_y of defect-free film is twice higher than the value G_x. The higher conductivity of the hybrid film in the direction of axis Y is explained by the contribution of the nanotube (10,0), which is current-conductive exactly along its axis. With the growth of the number of defects there is growth of electrical conductivity in both directions of current transport, which is related to the described above phenomena of electric charge transfer in the graphene-SWCNT (10,0)-graphene system. The difference also increases in the values G_x and G_y. Depending on the number of defects it is 2.5–3 times.

Table 2. Electrical conductivity of defect-free and defective hybrid graphene-SWCNT (10,0)-graphene film in direction of current transport zigzag (G_x) and armchair (G_y) of hexagonal lattice of graphene

Number of defects	G_x, μSm	G_y, μSm
0	25.3	51.2
1	40.3	121.3
2	42.1	154.2
3	59.5	159.6
4	75.2	167.9

Therefore, varying the number of defects of the single vacancy type, it is possible to reinforce the anisotropy of electrical conductivity in the hybrid graphene-SWCNT-graphene films, which is important for their potential use in the devices of semiconductor electronics, in particular, diodes and transistors.

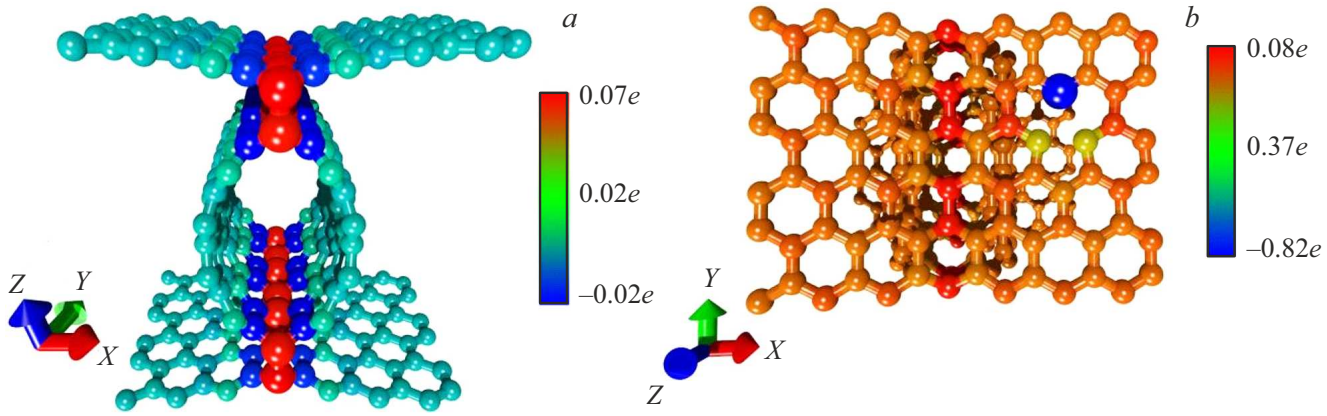

Figure 4. Distributions of partial charge by Mulliken for atoms of the super cells of defect free (*a*) and containing 1 defect of single vacancy type (*b*) in hybrid graphene-SWCNT (10,0)-graphene films. The electron charge is indicated as e on the color scale.

4. Conclusion

The patterns are established in the influence of the single vacancy defects at the electronic and electrophysical properties of quasi-2D hybrid graphene-SWCNT (10,0)-graphene films. If there are vacancy defects, the hybrid films preserve the energy gap between the valence band and conduction band provided for by the covalent nature of the bond between the graphene sheets and SWCNT, however, the value of the gap decreases 3 times (from 0.57 to 0.19 eV) as the number of defects increases from one to four. The appearance of the defects in the atomic lattice of the graphene reinforces the charge transfer between it and the SWCNT, in process of which the charge partially transfers from the nanotube to the graphene sheets, which causes growth of electric conductivity of hybrid graphene-nanotube films in both directions of current transport (zigzag and armchair of the hexagonal lattice of graphene) 3 times compared to the defect-free film. The presence of vacancy defects also strengthens anisotropy of electric conductivity in hybrid graphene-SWCNT (10,0)-graphene films, increasing the ratio of G_y/G_x from 2 to 3 times. The identified patterns indicate the possibility to control the electronic and electrophysical properties of quasi-2D hybrid carbon films due to the point defects, which must be taken into account when used in the devices of semiconductor nanoelectronics, including diodes and transistors.

Funding

The study was conducted with the support of the grant of the Russian Science Foundation (project No. 24-79-10316, https://rscf.ru/project/24-79-10316/, building atomistic models, study of the electronic and electrophysical properties of defect-free hybrid carbon nanostructures) and the state assignment of the Ministry of Education and Science of the Russian Federation (project FSRR-2023-0008, the study of the defect influence at the electronic and electrophysical properties of hybrid carbon nanostructures).

Conflict of interest

The author declares that he has no conflict of interest.

References

[1] O.S. Ayanda, A.O. Mmuoegbulam, O. Okezie, N.I. Durumin Iya, S.E. Mohammed, P.H. James, A.B. Muhammad, A.A. Unimke, S.A. Alim, S.M. Yahaya, A. Ojo, T.O. Adaramoye, S.K. Ekundayo, A. Abdullahi, H. Badamasi. J. Nanopart. Res. **26**, 106 (2024).

[2] Yu.A. Baimova, R.R. Mulyukov. Grafen, nanotrubki i drugie uglerodnye nanostruktury. RAN, M. (2018). 212 s. (in Russian).

[3] E.F. Sheka, L.A. Chernozatonsky, A.A. Artyukh. Pisma v ZhETF **89**, *7*, 412 (2009). (in Russian).

[4] A.A. Artyukh, L.A. Chernozatonskii, P.B. Sorokin. Phys. Status Solidi B **247**, *11–12*, 2927 (2010).

[5] V.T. Dang, D.D. Nguyen, T.T. Cao, P.H. Le, D.L. Tran, N.M. Phan, V.C. Nguyen. Adv. Nat. Sci.: Nanosci. Nanotechnol. **7**, *3*, 033002 (2016).

[6] W. Du, Z. Ahmed, Q. Wang, C. Yu, Z. Feng, G. Li, M. Zhang, C. Zhou, R. Senegor, C.Y. Yang. 2D Mater. **6**, *4*, 042005 (2019).

[7] A. Gbaguidi, S. Namilae, D. Kim. Nanotechnology **31**, *25*, 255704 (2020).

[8] J. Sheng, Z. Han, G. Jia, S. Zhu, Y. Xu, X. Zhang, Y. Yao, Y. Li. Adv. Funct. Mater. **33**, *43*, 2306785 (2023).

[9] I.N. Kholmanov, C.W. Magnuson, R. Piner, J.Y. Kim, A.E. Aliev, C. Tan, T.Y. Kim, A.A. Zakhidov, G. Sberveglieri, R.H. Baughman, R.S. Ruoff. Adv. Mater. **27**, 3053 (2015).

[10] S. Pyo, Y. Eun, J. Sim, K. Kim, J. Choi. Micro and Nano Syst. Lett. **10**, 9 (2022).

[11] B. Liu, J. Sun, J. Zhao, X. Yun. Adv. Compos. Hybrid Mater. **8**, 1 (2025).

[12] S. Wang, J. Yang, X. Zhou, J. Xie, L. Ma, B. Huang. J. Electroanal. Chem. **722**, 141 (2014).

[13] Z. Rezaei, M.R. Golobosnafard. J. Ultrafine Grained Nanostructured Mater. **55**, *1*, 45 (2022).

[14] M. Fikry, M. Abbas, A. Sayed, A. Nouh, A. Ibrahim, A.S. Mansour. J. Mater. Sci.: Mater. Electron. **83**, *7*, 391 (2022).

[15] G.K. Maron, J.H. Alano, B.d.S. Noremberg, L.d.S. Rodrigues, V. Stolojan, S.R.P. Silva, N.L. Villarreal Carreno. J. Alloys Compd. **836**, 155408 (2020).

[16] L. Chen, D. Li, X. Zheng, L. Chen, Y. Zhang, Z. Liang, J. Feng, P. Si, J. Lou, L. Ci. J. Electroanal. Chem. **842**, 74 (2019).

[17] J.P. John, M.N. T.E., B.S. T.K. Mater. Adv. **2**, 6816 (2021).

[18] R.T. Lv, E. Cruz-Silva, M. Terrones. ACS Nano **8**, *5*, 4061 (2014).

[19] K.L. Routray, S.J.D. Saha. Mater. Res. Bull. **150**, 111698 (2024).

[20] J. Cao, Y.X. Zou, X. Gong, P. Gou, J. Qian, R.J. Qian, Z.H. An. Appl. Phys. Lett. **113**, 061112 (2018).

[21] M. Alamri, B. Liu, C. Berrie, M. Walsh, J.Z. Wu. Nano Ex. **3**, *3*, 035004 (2020).

[22] S. Lepak-Kuc, K.Z. Milowska, S. Boncel, M. Szybowicz, A. Dychalska, I. Jozwik, K.K. Koziol, M. Jakubowska, A. Lekawa-Raus. ACS Appl. Mater. Interfaces. **11**, *36*, 33207 (2019).

[23] B.Yu. Valeev, A.N. Toksumakov, D.G. Kvashnin, L.A. Chernozatonsky. Pisma v ZhETF **115**, *2*, 103 (2022). (in Russian).

[24] J. Srivastava, A. Gaur. J. Chem. Phys. **155**, 244104 (2021).

[25] M.D. Bhatt, H. Kim, G. Kim. RSC Adv. **12**, *33*, 21520 (2022).

[26] V.V. Mitrofanov, M.M. Slepchenkov, G. Zhang, O.E. Glukhova. Carbon **115**, 803 (2017).

[27] M. Li, X.Liu, X. Zhao, F. Yang, X. Wang, Y. Li. Top. Curr. Chem. **375**, 29 (2017).

[28] M. Elstner, D. Porezag, G. Jungnickel, J. Elsner, M. Haugk, Th. Frauenheim, S. Suhai, G. Seifert. Phys. Rev. B **58**, *11*, 7260 (1998).

[29] B. Hourahine, B. Aradi, V. Blum, F. Bonafé, A. Buccheri, C. Camacho, C. Cevallos, M.Y. Deshaye, T. Dumitrică, A. Dominguez, S. Ehlert, M. Elstner, T. van der Heide, J. Hermann, S. Irle, J.J. Kranz, C. Köhler, T. Kowalczyk, T. Kubař, I.S. Lee, V. Lutsker, R.J. Maurer, S.K. Min, I. Mitchell, C. Negre, T.A. Niehaus, A.M.N. Niklasson, A.J. Page, A. Pecchia, G. Penazzi, M.P. Persson, J. Řezáč, C.G. Sánchez, M. Sternberg, M. Stöhr, F. Stuckenberg, A. Tkatchenko, V. W.-z. Yu, T. Frauenheim. J. Chem. Phys. **152**, 124101 (2020).
[30] A. Zobelli, V. Ivanovskaya, P. Wagner, I. Suarez-Martinez, A. Yaya, C. Ewels. Phys. Status Solidi B **249**, *2*, 276 (2012).
[31] R.S. Mulliken. J. Chem. Phys. **23**, 1833 (1955).
[32] S. Datta. *Quantum Transport: Atom to Transistor* (Cambridge University Press: Cambridge, London, UK, 2005), p. 404.

Translated by M.Verenikina